ELSEVIER

International Journal of Mass Spectrometry 223–224 (2003) 291–299

International Journal of Mass Spectrometry

www.elsevier.com/locate/ijms

Reactions of trapped ions with metal atoms: $O_2^+ + Ni$ and $NiN_2^+ + Ni$

Stephan Schlemmer*, Alfonz Luca, Dieter Gerlich

Faculty of Natural Science, University of Technology, 09107 Chemnitz, Germany

Received 11 March 2002; accepted 6 May 2002

Abstract

For studying reactions between ions and metal atoms, a temperature variable ring electrode trap (RET) has been combined with an atomic beam source. In Section 2, special attention is given to the calibration of the number density of the Ni atoms, injected along the axis of the trap from a metal evaporator. In Section 3, an unexpected isotope effect is reported for the reaction $O_2^+ + Ni \rightarrow NiO^+ + O$. The isotope ^{58}Ni reacts with a rate coefficient $k(670\,K) = (8 \pm 2) \times 10^{-10}\,cm^3\,s^{-1}$, whereas ^{60}Ni reacts two times slower. Formation of Ni_2^+ dimers by ternary reactions with He, H_2, and D_2 as buffer gas is very slow while, in the presence of N_2, efficient formation of Ni_2^+ has been observed via a catalytic cycle utilizing $Ni(N_2)_n^+$, $n = 1$–3, as intermediate. The rate coefficient for production of Ni_2^+ in collisions of NiN_2^+ with Ni has been determined to be $k(1060\,K) = (1.7 \pm 0.7) \times 10^{-10}\,cm^3\,s^{-1}$. (Int J Mass Spectrom 223–224 (2003) 291–299)

Keywords: Trapped ions; Metal atoms; Ring electrode trap

1. Introduction

Radicals play a key role in many cycles in nature such as atmospheric processes or chemistry of interstellar matter. Especially important are reactions of ions with metal atoms. The theoretical and experimental studies of such systems are still a challenge because of the open shell nature and technical difficulties, respectively. An early summary of rate coefficients from the sixties and seventies has been reviewed by Ferguson [1]. A combination of a Penning trap with a beam of sodium atoms is reported by Loch et al. [2]. The difficulty in obtaining absolute ion–metal atom cross-sections has been discussed by Levandier et al. [3]. In this study a high-temperature octopole/collision cell apparatus has been utilized for measuring integral cross-sections for charge transfer from Na to O_2^+, NO^+, and N_2^+. In order to derive thermally averaged rate coefficients, the cross-sections were extrapolated to thermal energies. This contribution reports thermal rate coefficients for the interaction of cold trapped ions with metal atoms from a high-temperature evaporation source.

Since the production of metal ions is easier using suitable ion sources [4], a lot of information comes from studies of reactions of metal ions and metalliferous compounds. Compared to the study of ion–metal atom reactions the chemistry of atomic transition-metal ions is very advanced. In mass

* Corresponding author.
E-mail: schlemmer@physik.tu-chemnitz.de

1387-3806/02/$ – see front matter
PII S1387-3806(02)00865-5

spectrometric studies using the guided ion beam or and ICR technique [5], the influence of the highly abundant electronically excited states and the role of the translational energy are the major facilities to unravel details of the dynamics of these reaction systems. Spin conservation is another consideration influencing the reaction pathways of metal ion–molecule collisions [5]. The lowering of the activation energy is the catalytic effect when metal and molecule approach each other (organometallic chemistry, surface science, and catalysis). That is a major driving force in this field. The large number of the transition metals and possible ligands present in nature make this field rather diverse especially when considering that solvation effects in metal–ligand complexes play an important role too.

One of the motivations of the present work was to grow covalently bound clusters by adding step-by-step single metal atoms. The rate coefficients of association depend strongly on the cluster size. In the first step, e.g., formation of the dimer, the lifetime of the collision complex is extremely small, in the order of a vibrational period. If the clusters reach a certain size, association can be considered as a sticking process, for which the probability may approach unity. In the case of metals, this may occur already at rather small number of atoms since many low lying electronic states can strongly influence the lifetimes of the collision complex. The association of weakly bound hydrogen cluster ions [6,7], and CO cluster ions [8,9] have been studied in detail using a 22-pole ion trap and the ring electrode trap (RET).

A thorough description of ion trapping techniques can be found in [10]. In most applications the neutral reactants are present as ambient gas in the trap. Using alternatively a beam of radicals or condensing atoms or molecules, passing through the trap, expands the flexibility of the apparatus. Since, for the first time, an atomic metal beam source is incorporated, Section 2 describes in detail the beam source and the calibration of the number density of the target in the trap. This procedure is essential for deriving absolute rate coefficients for reactions. Results for $O_2^+ + Ni$ and $NiN_2^+ + Ni$ are presented in the following.

2. Experimental

The experimental setup used for the study of reactions with Ni atoms is shown in Fig. 1. Its main functional units are a metal atom source, a RET, a quadrupole mass spectrometer (QMS), and an ion detector. The metal atom beam is generated by electron bombardment of the metal tip. Electrons emitted from the cathode are accelerated up to several kiloelectron-volt and hit the tip of the metal filament. At an electron current in the milliampere range, the metal tip is subject to several watts of heating power. Due to the poor heat conductivity of the filament and due to the small surface area of its tip, the metal can be heated up to its melting point. Considering the wide temperature range of the source, various materials can be evaporated. In this setup, only the

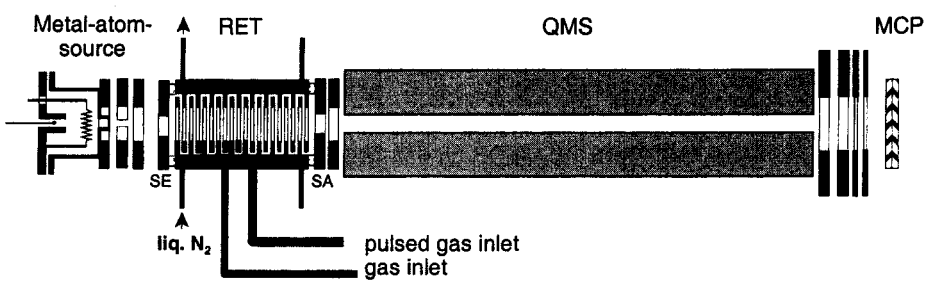

Fig. 1. Cross-sectional view of the ion trap apparatus. The central element is the RET which can be cooled to $T = 80$ K. Ions are produced either in the metal–atom-source and injected into the trap or inside the trap via ionization of neutrals. The beam of metal atoms is directed along the trap axis and interacts with the stored ions. After a variable reaction time product ions are extracted through the SA electrode, mass analyzed in QMS and counted via the MCP detector.

tip is heated to evaporation temperatures, therefore, the metal beam has the same purity as the filament material. More details of this miniature electron bombardment vaporization source can be found in [11]. Other metal beam sources with a similar principle of operation are commercially available.

In the present setup a Ni rod of 2.5 mm diameter with 99.997% purity [12] has been used. Upon vaporization, the Ni atoms are also under bombardment of the fast electron beam. As a consequence ions are also produced which can leave the source with high kinetic energies. They are slowed down and deflected by the adjacent electrodes shown in Fig. 1. In this way, out of the vapor beam, only neutral Ni atoms reach the ion trap region where collisions with stored ions are studied. The distance between the evaporating metal tip and center of the trap is 6 cm. By construction of the RET ceramic spacers of the pairs of electrodes are not subject to a metal beam deposition which enables a safe operation of the trap. Other interesting features of this particular trap have been described earlier [8,10,13]. In the present configuration a rf-voltage with an amplitude of 220 V and a frequency of 6.7 MHz has been used. Assuming a maximum kinetic energy of 0.1 eV, these conditions allow for storing singly charged ions in a mass range from 3 to 700 u within the adiabatic limit. The temperature of the RET is determined by a liquid medium flowing through the trap. Liquid nitrogen has been used presently. Due to wide field-free range of the trap, the ions are cooled down to the RET temperature [10]. The composition of the stored ion cloud is analyzed by the quadrupole mass filter (see Fig. 1). Transmitted ions are then detected with high efficiency by a multichannel plate detector (MCP) in Chevron arrangement followed by a conventional ion counting amplifier/discriminator setup.

The experiment is performed in a pulse mode. Primary ions are produced by electron bombardment of neutral atoms and molecules in the trap and by secondary reactions thereof. For this purpose electrons from the metal source are directed towards the trap applying a voltage pulse to the cup electrode of the source. In addition ions are continuously produced by VUV radiation caused by fast electrons hitting the metal tip. The ions are stored for a variable time (milliseconds up to minutes) and interact with the gas let in from the effusive gas inlets and/or with the metal atom beam. After a certain reaction time, the trap content is extracted by pulsing the gate electrode, SA, mass analyzed and detected. At the beginning of the each trapping cycle the rf-voltage is switched off to empty the trap. Due to excitation of the MCP by VUV, the electron beam is switched off during analysis of trap content. For the measurement of the temporal evolution of the ion cloud the cycle *ion production/trapping and reaction/analysis* is repeated several times for each product mass and the various trapping times.

From this evolution, rate coefficients of the associated reactions are determined. For this purpose the knowledge of density of the neutral collision partner, in the present case that of the neutral Ni atoms, is essential. It has been described by Nehasil et al. [11], that the Ni evaporation rate can be determined from the ionized part of the metal beam. We monitored the current of Ni ions, I_{Ni^+}, on the SE electrode, as a function of the heating power, P. The result of this calibration procedure is shown in Fig. 2. In order to maintain the same ionization conditions, i.e., the overlap of the electron beam and the evaporating Ni atoms inside the source, the acceleration voltage has been kept constant, $U = 2$ kV. The heating power has been controlled by varying the electron emission current, I_S. The ratio I_{Ni^+}/I_S, where I_S is current of electrons onto the metal tip, I_{Ni^+} is proportional to the Ni evaporation rate. Evaporation of Ni starts to be observable above a threshold of about 7 W (see Fig. 2), and increases exponentially with P, as indicated by the straight line in the semilog plot of Fig. 2. At smaller heating power a constant offset caused by electron bombardment ionization of rest gas and/or ionization due to energetic photons is dominant. The exponential increase has been used to calibrate the absolute number density of Ni atoms in the trap. For this purpose the absolute value of the evaporation rate has been derived from the material consumption. Considering the geometry of the vaporizing Ni filament and the homogeneous heating of its tip only, metal atoms

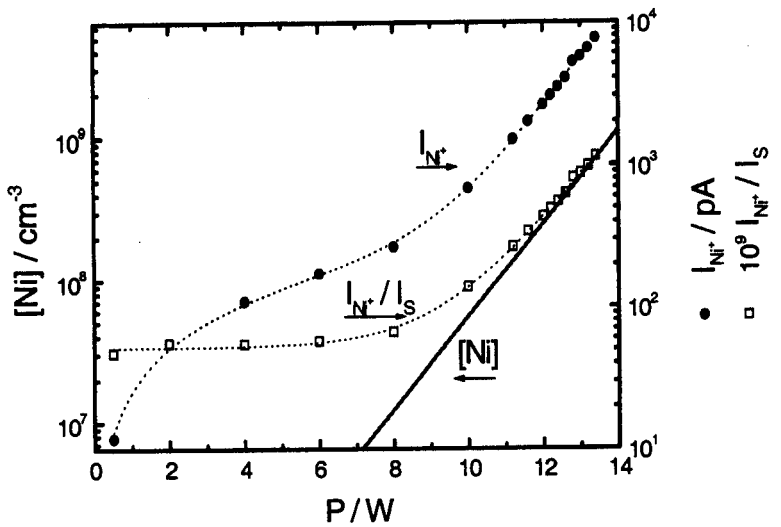

Fig. 2. Characterization of the metal beam. Ion current on SE electrode, I_{Ni^+} (●, right axis) is measured as a function of the heating power of the metal tip, which is controlled by the electron emission current I_S. For $P > 7$ W the number density of Ni atoms is proportional to I_{Ni^+}/I_S (□, right axis). It rises exponentially with increasing power, P. The exponential part (without offset) is plotted as a thick solid line and shows the Ni number density (left axis) in the middle of the RET. The calibration procedure is described in the text.

are vaporized isotropically into 2π sr and the average velocity is given by the evaporating temperature of Ni of ~1726 K (melting point). Under these conditions the number density at the center of the RET has been derived (see Fig. 2). Densities in the range from 10^7 to 10^9 cm^{-3} have been achieved. At typical rate coefficients for ion–molecule reactions of 10^{-9} cm^3 s^{-1} trapping times in the regime of seconds are required to detect the consumption of a major fraction of reactant molecules. At the highest evaporation rates of the metal source the material consumption is already quite high. For 10^9 cm^{-3} the 2.5 mm rod has to be moved at a velocity of about 5 μm min^{-1}. For a stable operation under these conditions an automatic movement is therefore mandatory. For the measurements presented here constant operation conditions over several minutes in each measurement were required. This could be achieved by manual translation of the metal rod in between measurements. Ni number densities in the measurements shown below were up to ~10^8 cm^{-3}.

The motion of the ions, A^+, and the nickel neutrals is characterized by different Maxwellian distributions at temperatures T_{A^+} and T_{Ni}. The effective collision temperature is given by $T = \mu(T_{A^+}/m_{A^+} + T_{Ni}/m_{Ni})$, where μ is the reduced mass. The ions are cooled down by collisions with buffer gas to 100 ± 20 K. The temperature of the metal atoms, T_{Ni}, is defined by the temperature of the metal tip. For this temperature we assume the melting temperature T_{Ni} = 1700 ± 100 K, because the cylindrical Ni rod forms a droplet shaped tip during operation. Accordingly the reaction temperature for O_2^+ + Ni collisions is 670 ± 120 K and for NiN_2^+ + Ni collisions 1060 ± 100 K.

3. Results and discussion

3.1. $O_2^+ + Ni$

As a first reaction system collisions between O_2^+ and Ni atoms have been studied. Two product channels have to be considered in a bimolecular collision.

$$O_2^+ + Ni \rightarrow NiO^+ + O, \quad (1a)$$

$$O_2^+ + Ni \rightarrow Ni^+ + O_2. \quad (1b)$$

Both are highly exothermic, reaction (1a) ΔH_0 = −31.6 kcal mol^{-1}, reaction (1b) ΔH_0 = −102.8 kcal mol^{-1}.

O_2^+ ions have been produced in the trap. In order to minimize oxidizing reactions, especially the formation of neutral NiO, and other influences in the nearby metal source due to the presence of O_2 a dedicated O_2^+ production scheme has been used. O_2 and He have been let in the trap via a continuous and a pulsed gas inlet, respectively. The pulsed inlet operates synchronously with the electron pulse from the metal source. With an excess of He, He^+ are the majority of ions produced. In a fast charge transfer reaction with the ambient neutral O_2, O_2^+ ions are formed more readily than by the initial electron bombardment. Therefore much lower O_2 densities ($[O_2] < 5 \times 10^9\,cm^{-3}$) are necessary. Due to the fact that outside the trap the O_2 number density is even lower by a factor of about 200, the contamination of the metal tip is negligible. For the determination of the rate coefficients for reaction (1) the temporal evolution of stored ions has been measured. A typical example is shown in Fig. 3. O_2^+ ions are produced during the first 0.5 s, not shown in Fig. 3 due to the rapid changes of neutral gas density. During the following 1.3 s the number of O_2^+ primary ions as well as Ni^+ and NiO^+ products are recorded. The number of O_2^+ ions is derived from the number of detected $^{18}O^{16}O^+$ since the large amount of $^{16}O_2^+$ ions would saturate the detector. The two most abundant isotopes of Ni (^{60}Ni and ^{58}Ni) have been detected in both product channels. The number of products increases linearly with time while the number of reactants decreases. Ni^+ ions are formed via the charge transfer reaction (1b) and also due to constant photoionization of Ni neutrals in the trap. A fraction of the Ni^+ products can escape the trap because of their high kinetic energy. Therefore we do not determine a net rate coefficient for the Ni^+ production. A possible secondary reaction of Ni^+ is $Ni^+ + O_2 \rightarrow NiO^+ + O$. This reaction is endothermic by $\Delta H_0 = 53.6\,kcal\,mol^{-1}$ [14] and can be neglected in the present case. In order to exclude possible modifications of the tip surface due to O_2 gas and contamination of Ni atom beam by oxides some other test procedures have been undertaken [15]. For instance the number of primary O_2^+ ions has been varied by varying the He number density in the pulse while $[O_2]$ has been kept constant. From this it turns out that the production rate of NiO^+ ions is proportional to the number of stored O_2^+ ions.

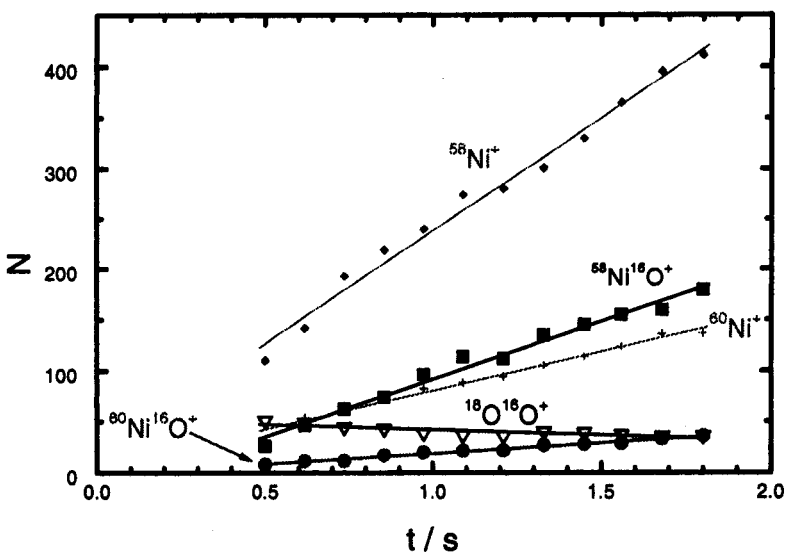

Fig. 3. Temporal evolution of stored ions at 80 K and at number densities of $[O_2] = 5 \times 10^9\,cm^{-3}$ and $[Ni] = 6.2 \times 10^7\,cm^{-3}$. Primary O_2^+ ions, detected via the less abundant $^{18}O^{16}O^+$ isotopomer (4×10^{-3}), are produced via ionization of He gas (from a pulsed gas inlet) following the charge transfer reaction with O_2. O_2^+ ions react with Ni neutrals and form NiO^+ and Ni^+ products. Solid lines represent linear fits to the temporal evolution from which rate coefficients are determined.

In order to derive a rate coefficient from the number of products one has to make sure that no products are lost. Since reaction (1a) is highly exothermic, products are formed with high kinetic energy. Assuming that all exothermicity is transferred to the kinetic energy of products, NiO^+ ions can leave the reaction with a maximum kinetic energy of 0.24 eV. In the present trap experiment NiO^+ product ions with up to 1.1 eV can be stored safely. Therefore no products are lost under the current experimental conditions.

From analysis of the constant production rate of NiO^+ (seen in Fig. 3), rate coefficients for reaction (1a) have been determined for the two nickel isomers, ^{58}Ni and ^{60}Ni. Results are plotted in Fig. 4 as function of Ni number density. Within the given error limits the rate coefficients are constant and the average values are $k_{1a}(^{58}Ni) = (8 \pm 2) \times 10^{-10}\,cm^3\,s^{-1}$ and $k_{1a}(^{60}Ni) = (4 \pm 1) \times 10^{-10}\,cm^3\,s^{-1}$. The error margins include statistical deviations. Possible systematic errors in the determination of the Ni number density of about 50% (see Section 2), are not included. Besides the Ni density the actual temperature of the Ni atoms, T_{Ni}, also varies slightly with the heating power of the tip (~10%). This effect could lead to an additional statistical error in k, provided there exists an activation barrier along the reaction path which height is comparable to the reaction temperature. The rate coefficients for reaction (1a) make up a large fraction of the Langevin rate coefficient $k_L = 1.3 \times 10^{-9}\,cm^3\,s^{-1}$. Therefore no substantial barrier is hindering the reaction.

Photoionization of the neutral Ni atoms is the dominant Ni^+ production mechanism. Therefore the ratio of $^{58}Ni^+$ to $^{60}Ni^+$ is an approximate measure of the ^{58}Ni to ^{60}Ni abundance ratio in the atomic beam of neutrals. Within errors this ratio, 2.97 ± 0.30, corresponds to the natural abundance of these two isotopes, $0.681/0.262 = 2.60$. For the same reason, however, no reliable rate coefficients for the electron transfer channel, reaction (1b), could be determined. Nevertheless the charge transfer channel seems to play a certain role in this collision system. Due to the long range nature of the charge transfer process both reaction pathways may start with a period of sharing the electron. For the exchange of an O-atom a more intimate approach is necessary. However, once the atom is exchanged reaction proceeds along path (1a). In this picture most likely channels (1a) and (1b) are in competition in reaction (1). Assuming no barrier for these two highly exothermic product channels, reaction is happening at collision rate and the sum of both rate coefficients adds

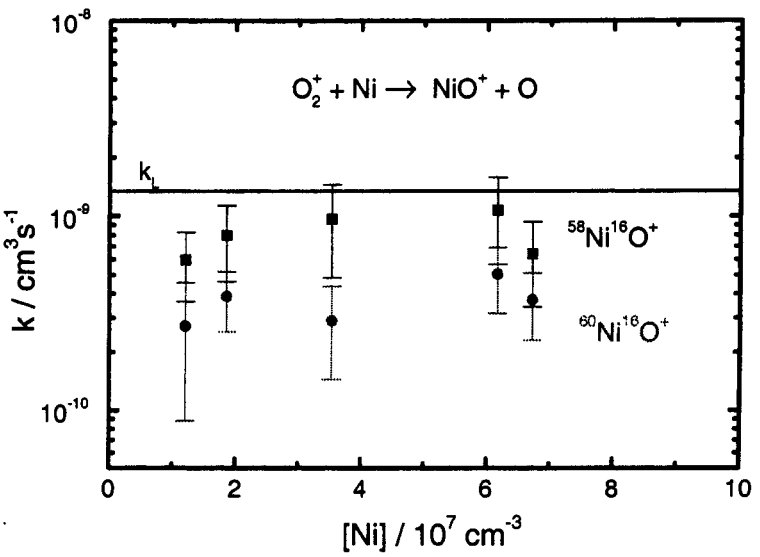

Fig. 4. Rate coefficients for $^{58}NiO^+$ and $^{60}NiO^+$ formation in $O_2^+ + Ni$ reaction. Within the indicated errors the rate coefficients are independent on the Ni number density as expected for a bimolecular process. The Langevin rate coefficient, k_L, is marked by a horizontal line.

up to the Langevin rate coefficient. From this assumption the rate coefficients for the charge transfer channel can be estimated to be $k_{1b}(^{58}Ni) = 5 \times 10^{-10}\,cm^3\,s^{-1}$ and $k_{1b}(^{60}Ni) = 9 \times 10^{-10}\,cm^3\,s^{-1}$.

Reaction (1) shows a rather strong isotope effect, i.e., the lighter ^{58}Ni isotope forms NiO^+ ions at twice the rate than ^{60}Ni. Such isotope effects can have different origins. Different nuclear spins of the different isotopes can play a role in the formation of products. However, in the case of ^{58}Ni and ^{60}Ni the nuclear spins are the same. Differences in zero point energy due to the different masses of the atoms can be important for the formation of isotopomers, known as isotopic fractionation. The lighter the species the stronger this effect usually is. Since the mass difference for the two Ni isotopes are very small an isotope effect of this size is unexpected. An isotope effect of similar strength has been reported for the rate coefficients of formation and destruction of ozone [16], where the mass differences are also relatively small when compared to light hydrogen/deuterium containing species where these effects are the strongest. In summary the isotope effect is quite surprising. In view of the possible competition between reactions (1a) and (1b) and its common entrance channel of sharing the electron small differences in the dynamics may, however, lead to substantial changes in the branching ratio of the two channels.

3.2. $NiN_2^+ + Ni$

One aim of combining a neutral atomic beam source, here of metal atom M, with an ion trap experiment is to study the kinetics and dynamics of formation of covalently bound agglomerates, M_n^+, in associative collisions. The most common way of production is ternary association [9,17]

$$M_n^+ + M + X \rightarrow M_{n+1}^+ + X. \quad (2)$$

This is a sequential process in which M_n^+ and M form a collision complex, M_{n+1}^{+*}, and the collision with an atom or molecule, X, leads to stabilization of the molecular ion M_{n+1}^+. Considering the maximum number density of Ni, $\sim 10^9\,cm^{-3}$, as well as manageable densities, $[X] \sim 10^{14}\,cm^{-3}$, ternary rate coefficients larger than $10^{-26}\,cm^{-6}\,s^{-1}$, can be determined during a $\Delta t = 10\,s$ trapping time and a minimum detection limit of $\Delta[M_{n+1}^+]/[M_n^+] \sim 0.01$. Corresponding lifetimes of the collision complex, M_{n+1}^{+*}, as short as 1 ns are measurable with the current setup, assuming a stabilization efficiency of $\beta = 1$. In the present case formation of the smallest Ni cluster, Ni_2^+, could not be detected following reaction (2). This implies that the corresponding ternary rate coefficient is smaller than the above limit and the corresponding complex lifetime is shorter. This is not surprising since for the association of two atoms ternary rate coefficients are typically in the range of 10^{-31} to $10^{-27}\,cm^{-6}\,s^{-1}$. For that reason different routes for the formation of Ni cluster ions have been investigated.

Catalytic formation of Ni_2^+ has been found in the following two-step reaction scheme

$$Ni^+ + 2N_2 \rightarrow NiN_2^+ + N_2, \quad (3)$$

$$NiN_2^+ + Ni \rightarrow Ni_2^+ + N_2. \quad (4)$$

In the first step NiN_2^+ is formed in ternary association of Ni^+ and N_2. NiN_2^+ has a strong binding energy of $23.7\,kcal\,mol^{-1}$ [18], when compared to the collision energy in the trap experiment. In the second reaction N_2 is replaced by Ni. The Ni_2^+ product is bound about two times tighter, $2.08\,eV = 47.9\,kcal\,mol^{-1}$ [19], than NiN_2^+. It is an interesting question whether the exothermic reaction (4) is happening without barrier.

For the study of this reaction system N_2 has been let in the trap at a number density in the range of 3×10^{12} to $1 \times 10^{14}\,cm^3$. At the beginning of each trapping cycle the rf-voltage is turned off and the trap is emptied. Ni from the metal atom source, $[Ni] = 3 \times 10^8\,cm^{-3}$, and N_2 are subject to the continuous ionizing radiation of the metal source such that N^+, N_2^+, and Ni^+ are formed at a constant rate. A typical result is shown in Fig. 5. The number of stored ions is displayed as a function of the trapping time in a double logarithmic plot. The number of Ni^+ ions increases linearly, solid line in Fig. 5, as expected for a constant production rate. Again a less abundant isotope, $^{64}Ni^+$,

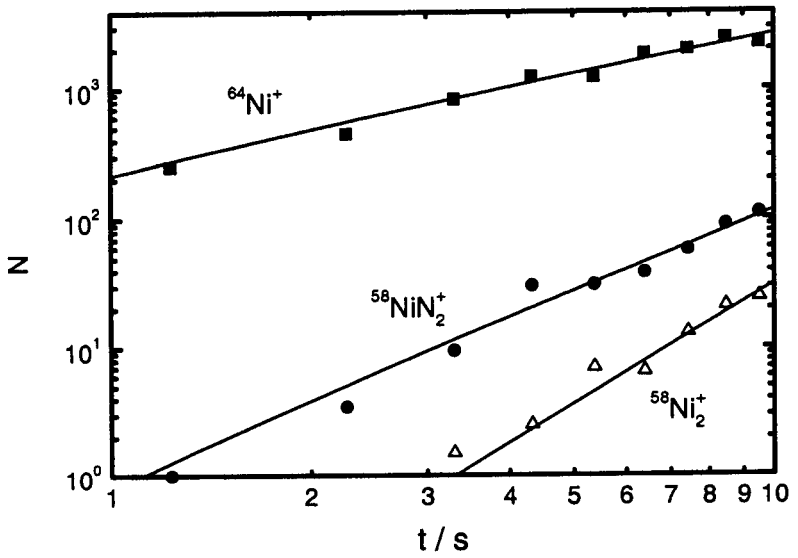

Fig. 5. Double logarithmic plot of the temporal evolution of stored ions at 80 K and at number densities $[N_2] = 7 \times 10^{12}\,cm^{-3}$ and $[Ni] = 2.6 \times 10^{8}\,cm^{-3}$. Primary ions are produced at a constant rate via continuous ionization of neutrals in the trap. Straight line dependencies with different slopes demonstrate linear, quadratic and cubic formation of primary Ni^+ ions, NiN_2^+ products (reaction (3)) and Ni_2^+ secondary products (reaction (4)) respectively. Solid lines represent best fit approximations from which the rate coefficient for the formation of Ni_2^+ is derived.

has been detected in order to avoid saturation effects of the detector. The number of NiN_2^+, the product of reaction (3), increases quadratic with trapping time, solid line in Fig. 5. This behavior is expected as the number of Ni^+ reactants increases already linearly in time. As a consequence the number of Ni_2^+ products, reaction (4), increases as the third power of time. This result is consistent with the proposed reaction scheme.

In order to determine the rate coefficients for reactions (3) and (4), possible other formation pathways for Ni_2^+ have to be explored. For this purpose the N_2 number density has been varied. At low densities, $10^{12}\,cm^{-3}$, association products N_3^+, N_4^+, NiN_2^+ are observed. The number of NiN_2^+ products increases quadratically as in Fig. 5. The consumption of NiN_2^+ via secondary reactions is very low. At higher number densities, $>5 \times 10^{12}\,cm^{-3}$, also NiN_4^+ and NiN_6^+ clusters are produced via ternary association. Reliable rate coefficients for these processes could not be determined due to the possible influence of the metal atom source. In the case of X = He, H_2 and D_2 as a buffer gas, NiX_n^+ cluster ions have not been found in the mass spectra. In principle Ni_2^+ can be formed in secondary reactions with $Ni(N_2)_n^+$, $n = 2, 3$, cluster ions too. However, the amount of NiN_4^+ and NiN_6^+ clusters is too small to form the observed quantity of Ni_2^+ at a reliable rate. Therefore we conclude that Ni_2^+ in Fig. 5 is almost exclusively produced via reactions (3) and (4) and rate coefficients can be determined from the ordinate value in the double logarithmic plot.

As the production of NiN_2^+ ions in the metal source can not be excluded, the rate coefficient for NiN_2^+ formation could not be determined. The rate coefficient for reaction (4) shows a slight increase with $[N_2]$. However, this trend is still in the range of the statistical error. The average value of the rate coefficient is $k_3 = (1.7 \pm 0.7) \times 10^{-10}\,cm^3\,s^{-1}$. This value is approximately six times smaller than the Langevin rate coefficient for the $NiN_2^+ + Ni$ collision system, $k_L = 1.1 \times 10^{-9}\,cm^3\,s^{-1}$. This is an interesting result since it indicates that reaction (4), although very exothermic, is not at all proceeding at collision rate. Several dynamical restrictions could be responsible for this finding. Information about the structure and energetics of the $(Ni_2N_2)^+$ complex would be very helpful in understanding the current result.

4. Conclusion

The combination of a metal atom beam source and an ion trap apparatus (RET) allows new kind of experiments, the collision of neutral metal atoms with high evaporation temperature and atomic or molecular ions, $I^+ + M$. Such collision systems are complementary to the more commonly studied $M^+ + I$ systems. As a first example results from the reaction $O_2^+ + Ni$ can be compared to the systematically studied $Ni^+ + O_2$ case.

The metal atom beam source has been characterized and densities up to $10^9\ cm^{-3}$ can be obtained routinely. These densities suit well with the conditions necessary to determine typical bimolecular rate coefficients in a trap experiment. Combination with additional buffer gas at high densities shows that also ternary rate coefficients as small as $10^{-26}\ cm^6\ s^{-1}$ can be measured with the present compact and simple setup. For less likely processes a more advanced metal atom source with higher evaporation rate employing an automatic translation of the metal filament should be built. The Ni_2^+ dimer ion has been produced even at small Ni densities using a catalytic cycle reaction. Different ways of vaporizing metals should be considered when ionizing radiation from the source is not tolerable.

The present experimental setup was built with emphasis on simplicity and compactness. Separation of ion production, neutral beam source and trap region will make the use of the combination and the analysis of the data much easier as compared to the present study. A new setup with an ion source oriented transverse to the trap axis and a differentially pumped source region along the axis is used today [20]. This allows a clean operation of the beam source and high flexibility for the ion production.

Acknowledgements

The development of the presented method was supported by the VW foundation within the program of *Intra- und Intermolekulare Elektronenübertragung*. A.L. thanks the VW foundation for a scholarship as well as V. Nehasil and V. Matolin for technical support with the metal source.

References

[1] E.E. Ferguson, Radio Sci. 7 (1972) 397.
[2] R. Loch, R. Stengler, G. Werth, J. Chem. Phys. 91 (1989) 2321.
[3] D.J. Levandier, R.A. Dressler, E. Murad, Rev. Sci. Instrum. 68 (1997) 64;
D.J. Levandier, R.A. Dressler, S. Williams, E. Murad, J. Chem. Soc. Faraday Trans. 93 (1997) 2611.
[4] P.B. Armentrout, Annu. Rev. Phys. Chem. 41 (1990) 313.
[5] P.B. Armentrout, J.L. Beauchamp, Acc. Chem. Res. 22 (1989) 315.
[6] W. Paul, B. Lücke, S. Schlemmer, D. Gerlich, Int. J. Mass Spectrom. Ion Process. 150 (1995) 373.
[7] W. Paul, S. Schlemmer, B. Lücke, D. Gerlich, Chem. Phys. 209 (1996) 265.
[8] A. Luca, S. Schlemmer, I. Cermák, D. Gerlich, Rev. Sci. Instrum. 72 (2001) 2900.
[9] S. Schlemmer, A. Luca, J. Glosik, D. Gerlich, J. Chem. Phys. 116 (2002) 4508.
[10] D. Gerlich, Adv. Chem. Phys. LXXXII (1992) 1.
[11] V. Nehasil, K. Masek, O. Moreau, V. Matolin, Czech. J. Phys. 47 (1997) 261.
[12] A. Aesar, Johnson Matthey GmbH, Zeppelinstr. 7, D-76185 Karlsruhe.
[13] D. Gerlich, G. Kaefer, Ap. J. 347 (1989) 849.
[14] E.R. Fisher, J.L. Elkind, D.E. Clemmer, R. Georgiadis, S.K. Loh, N. Aristov, L.S. Sunderlin, P.B. Armentrout, J. Phys. Chem. 93 (1990) 2676.
[15] A. Luca, Ph.D. thesis, Technical University Chemnitz, April 2001, http://archiv.tu-chemnitz.de/pub/2001/0046/index.html.
[16] S. Wolf, M. Bitter, D. Krankowsky, K. Mauersberger, J. Chem. Phys. 113 (2000) 2684.
[17] R.G. Keesee, A.W. Castleman Jr., J. Phys. Chem. Ref. Data 15 (1986) 1009.
[18] C.W. Bauschlicher Jr., S.R. Langhoff, L.A. Barnes, Chem. Phys. 129 (1989) 431.
[19] L. Lian, C.-X. Su, P.B. Armentrout, Chem. Phys. Lett. 180 (1991) 168.
[20] A. Luca, D. Voulot, D. Gerlich, in: J. Safrankova (Ed.), 11th Annual Conference of Doctoral Students: June 11, 2000 to June 14, 2002, Physics of Plasmas and Ionised Media, MATFYZPRESS, Prague, 2002.